Full Paper | http://dx.doi.org/10.17807/orbital.v13i1.1577

Morphology and Corrosion Behavior Study of Thin TiN Films Deposited at Different Substrates by DC Magnetron Sputtering

B. Abdallah*, M. Kakhia, W. Alsadat, W. Zetun, A. Hijazy

TiN thin films have been deposited by magnetron sputtering (DC) method under pure argon (100% Ar) gas for different times at 100 °C temperature. Additionally, three substrate types have been used: Low Carbon Steel (LCS), Stainless Steel (SS304) and Silicon of (100) orientation. The composition of the films has been verified by Energy Depressive X-ray Spectroscopy (EDX) analysis for films deposited on Si substrate. This analysis has proved that the nitride films TiN was sub stoichiometry, Scanning Electron Microscope (SEM) image was used to estimate the thickness of TiN/Si film. X-ray diffraction (XRD) measurements were also applied to investigate the orientations of films. All the films (coated samples) have shown enhanced corrosion resistance compared with virgin SS304 and LCS substrate (noncoated sample) in 3.5% NaCl at 25 °C (equivalent to seawater). Morphological behavior was investigated by means of Atomic Force Microscopy (AFM), which indicates very smooth films and consequently related with corrosion resistance using Tafel and the electrochemical impedance spectroscopy (EIS) measurements. It was found the thinner film has revealed higher corrosion resistance and low roughness.

Graphical abstract

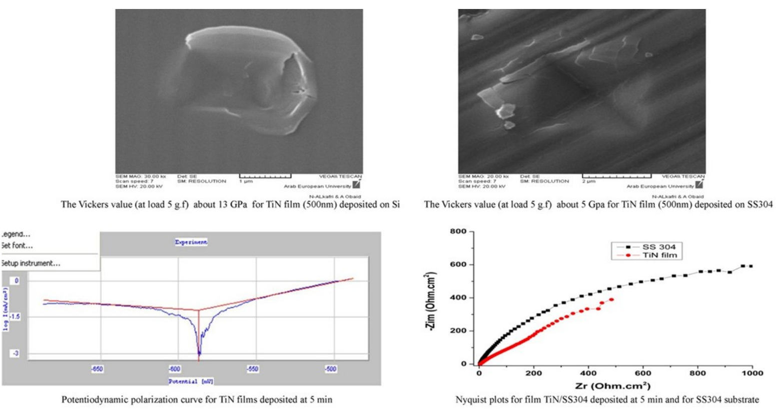

Keywords

TiN film
DC magnetron sputtering
Morphology
Corrosion behavior

Article history

Received 06 December 2020
Revised 25 January 2021
Accepted 25 January 2021
Available online 30 March 2021

Editor: Adilson Beatriz

1. Introduction

Titanium alloys are widely utilized for variety of applications, and have not been comprehensively investigated [1, 2], so the new researches are needed. Owing to their well-known interesting chemical and mechanical properties [3] compared with pure titanium. The titanium element is a monophase metal, physiologically inert, and non-toxic. Few studies have been performed on this alloy as thin film, in previous work, we have demonstrated a successful preparation of TiAlV films by vacuum arc discharge system [4] and by magnetron sputtering [5]. Most

Atomic Energy Commission, Department of Physics, P. O. Box 6091, Damascus, Syria. *Corresponding author. E-mail: **pscientific27@aec.org.sy**

applications of titanium involve nitriding of this metal [6] enhanced mechanical properties, high resistance to corrosion and wear and good hardness and tenacity [7]. On the other view, mechanical properties such as corrosion behavior and microhardness are related to the deposition method, vacuum arc deposition technique [4]. This arises due to the difference deposition techniques, Subramanian et al. [8] corrosion performance study indicated that the Ti0.5Al0.5N film had better corrosion resistance when compared to TiN and AlN coated substrates. We have found in a provirus work, TiN thin films by vacuum arc discharge method have been prepared at different conditions [4, 9]. The formation of "protective" oxide-TiO_2 layer on the surface of film results in excellent corrosion resistance in various test solutions and physiological media [5]. Other preparation techniques have also been used to deposit thin titanium nitride films (TiAlVN and TiN), for example chemical vapor deposition (CVD) or physical vapor deposition (PVD) such as vacuum arc deposition to obtain ZrNx [10] and TiN/ZrN [11] multilayers films, pulsed laser deposition (PLD) [12] and magnetron sputtering RF [13] or DC [14], where mechanical properties, structural and composition were studied. Magnetron sputtering [15] is widely used in the manufacturing technology of metal nitride such as CrN [16], NbN and TiN, because of producing high quality films with controlled thickness and morphology [17]. Plasma conditions and deposition parameters such as substrate temperature, deposition time or thickness, power and oxygen partial pressure [18] influence the physical (structural and optical) properties of thin films have already been studied in previous work [15, 18].

In this work, TiN films have been deposited on Si, LCS and SS304 substrates by DC magnetron sputtering. The crystallographic properties of the films were studied by XRD technique. The microhardness was investigated using Vickers method. In addition, the elemental composition of the films was obtained by EDX techniques. AFM, SEM and optical microscope were used to reveal the morphology and value of roughness for thin films. The corrosion performance was investigated in seawater (3.5% NaCl at 25°C) using potentiodynamic polarization and EIS measurements.

2. Material and Methods

The films were prepared by a DC magnetron sputtering method beginning from high pure (99.99%) TiN target (50 mm diameter) was used for preparation of TiN film in pure argon plasma. The films synthesized for 75 w at 100 °C deposited on Si (100) and LCS substrates at different deposition time (varied 5, 10, 15 and 20 min). A cylindrical high-vacuum chamber was fabricated locally [19]. The residual pressure was lower than 2.10^{-6} Torr, and the working pressure was about 4 mTorr.

SEM -Tescan Vega II XMU used to measure the thickness and indentions dimension. Energy Depressive X-ray Spectroscopy (EDX) used for determination of the elemental composition. Microhardness measurements were performed using an HX-1000 micro-hardness tester with Vickers indenter at loading force of 5 gram force. The electrochemical corrosion analysis was carried out using classical cell by means of Voltalab PGZ 301 system (France) of 300 mL capacity. The electrodes used in the cell are working electrode (the sample). The studies were carried out in seawater (3.5% NaCl solution) at 25±1 °C with electrode potential was raised from -800 mV to 1000 mV. The critical parameters of corrosion like E_{corr}, and I_{corr} and were evaluated from the Tafel plots. In the EIS measurement, at its corrosion potential (E_{corr}) (100 KHz to100 mHz frequency range) and the rotation speed of the working electrode was 100 rpm.

3. Results and Discussion

3.1 SEM characterization (Cross sectionandMicrohardness)

Figure 1 (a and b) shows SEM cross-sectional images for TiN thin films on silicon substrate, where the thickens were varied from 125 nm to 500 nm with increase the deposition time from 5 min to 20 min, respectively. The average deposition rate was about 25 nm/min (thickness/time). Also, SEM images were utilized for measure the diameters of diamond and calculate the Vickers's hardness (at load 5 g.f) for thicker film (500 nm), where (c) and (d) deposited on Si substrate and SS304 substrate, respectively. The Vickers value was about 13 GPa for TiN film deposited on Si and was about 5 GPa for film deposited on SS304. Its importance to indicate that the measured value is composite hardness (TiN on substrate not pure hardness), where this Microhardness for TiN film was higher than value of substrates (HV_{Si} = 6 GPa and HV_{SS304}=2.5 GPa).

Danisman et al. [20] have found that the cutting conditions were very changeable in drilling operations, further machining tests have to be done to understand the wear properties of these coatings (TiN, TiAlN) best. We found in previous work [19] that increasing the current to improve film quality (bigger grain size), and consequently has been influence to mechanical and corrosion properties Ti6Al4V/SS304 film. TiAlN film has higher hardness value than TiN film [14]. The difference in hardness values for films depend on many parameters (load, substrate, composition, …) and in fact adding, the element to nitride films increase the hardness and influence to all behaviors could be that due to strain and modification of the structure (grain size or phase type cubic/hexagonal) [14]. on another hand, mechanical properties such as stress and microhardness relate of the deposition method [4, 19]. Abdallah et al. [4] prepared TiAlV films by vacuum arc deposition, the microhardness varied from 18.1 GPa to 15.2 GPa with increase the temperature from 50 °C to 400 °C.

3.2 Morphologycharacterization (AFM)

Figure 2 show AFM images for (a) 2D, (b) 3D for 1x1 µm area, (c) 2D and (d) 3D for 200x200 nm area of TiN/Si deposited at 5 min. Also, (e) 2D and (f) for 1x1 µm, (g) 2D and (h) 3D for 200x200 nm area of TiN/Si fim deposited at 10 min. The RMS (Root mean square roughness) value was less than 1nm (0.7 nm and 0.5 nm) for thin TiN/Si films deposited at 5 and 10 min. It was interesting to note that the RMS had small value, indicates that the films was smooth due to nature of the sputtering method or/and due to the TiN target was sputtered as atoms not molecule.

It has been found that the surface microstructure of the film and the size of grain have remarkable effects on the corrosion resistance [21]. Similarly, Figure 3 presents AFM images for (a) 2D, (b) 3D for 1x1 µm area, (c) 2D and (d) 3D for 200x200 nm area of TiN/Si deposited at 15 min. Also, (e) 2D and (f) for 1x1 µm, (g) 2D and (h) 3D for 200x200 area of TiN/Si film deposited at 20 min. The roughness increases from 1.7 nm to 2.5 nm with increase the deposition time

from 15 min to 20 min (with increase the thickness to 500 nm for 20 min time). This phenomenon was observe where the thickness increase for AlN film [17], ZnO film [22] deposited by magnetron sputtering in previous work.

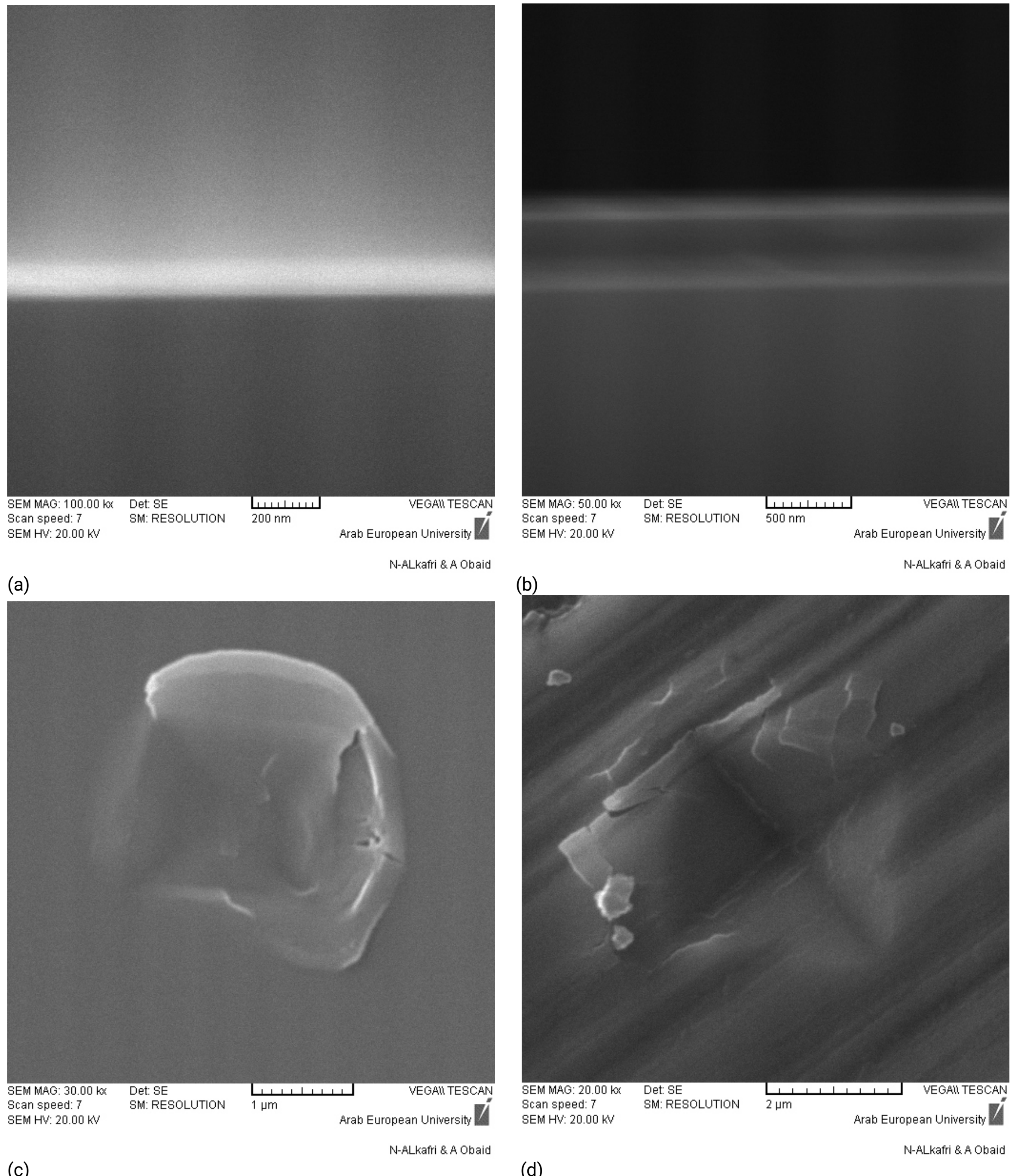

Fig. 1. SEM cross section images (a) thinner and (b) thicker films deposited with on Si substrate. SEM surface view for (c) TiN/Si and (d) TiN/SS304 at 5 g.f.

The morphology of the surface (roughness, size, form and nanostructure) affects the mechanical, physical, elementary contain and electrical properties of thin films comparative to the bulk performance [23].

3.3 XRD study

Figure 4 shows four XRD patterns of the prepared TiN films on Si(100) substrates at different deposition times. The films were amorphous for film deposited for 5 min, and become crystallized with increase the time, where their XRD patterns show a structure close to TiN (NaCl-structure) with two peaks characteristic of cubic phase, corresponding to (111) and (200) orientation at about 36.9° and 42.1°, respectively [19]. The increase of the peak intensity (especially for (111) preferred orientation) can be correlated with increase the thickness due to increase of deposition time.

The grain size for (111) orientation, using Scherrer's equation, increased from 0 nm to 13 nm with increase the deposition time from 5 min to 20 min. This improvement of the quality crystalline could arise due to increase the thickness of the deposition of TiN on silicon substrate**.** This behavior was observed in previous work using magnetron sputtering [17].

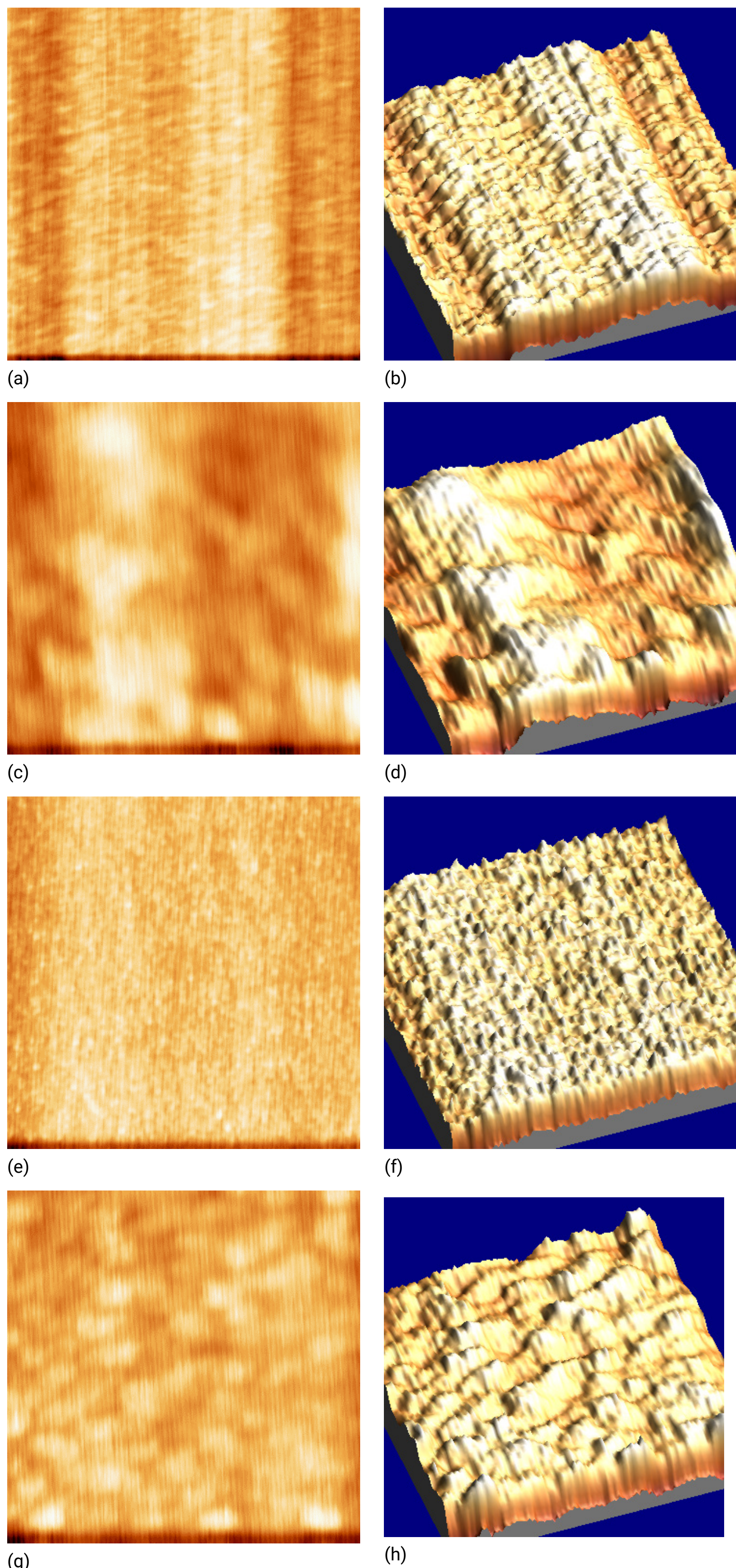

Fig. 2. AFM images for (a) 2D, (b) 3D for 1x1 μm area, (c) 2D and (d) 3D for 200x200 nm area of TiN/Si deposited at 5 min. also, (e) 2D and (f) for 1x1 μm, (g) 2D and (h) 3D for 200x200 area of TiN/Si film deposited at 10 min.

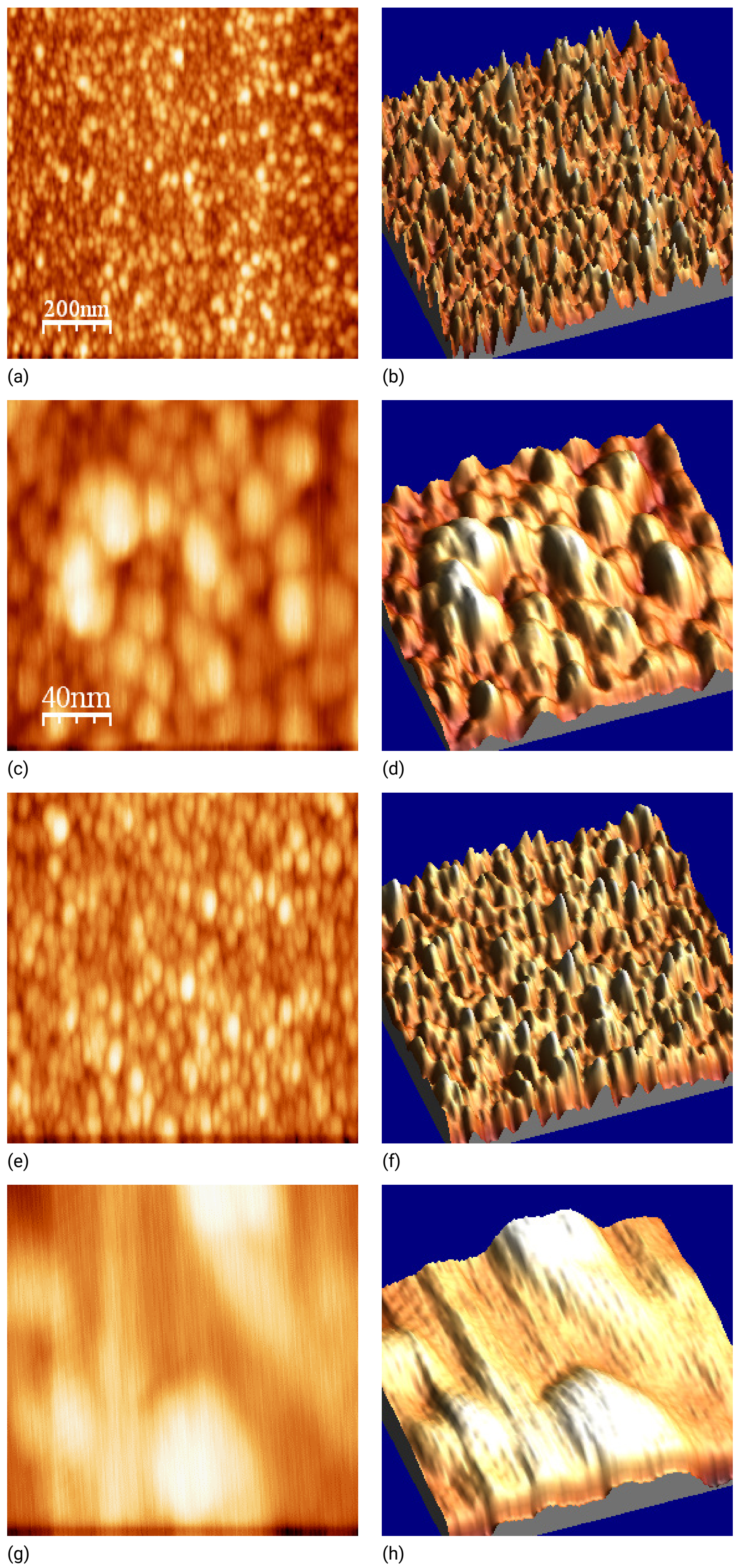

Fig. 3. AFM images for (a) 2D, (b) 3D for 1x1 μm area, (c) 2D and (d) 3D for 200x200 nm area of TiN/Si deposited at 5 min. also, (e) 2D and (f) for 1x1 μm, (g) 2D and (h) 3D for 200x200 area of TiN/Si film deposited at 10 min.

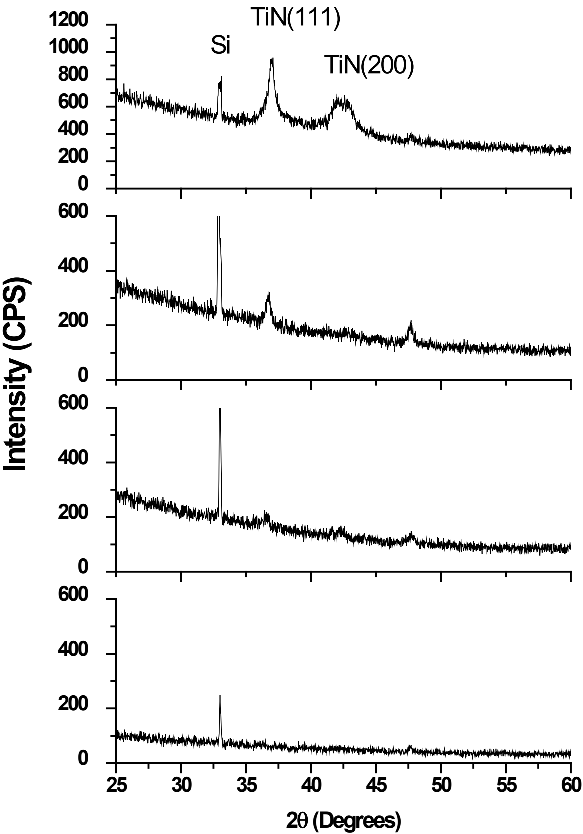

Fig. 4. Four XRD patterns of the prepared TiN films on Si(100) substrates at different deposition time.

3.4 EDX characterization

The composition of the two TiN/Si films was examined by means of EDX as shown in Figure 5. X-ray peaks correspond to Ti and N elements present in the TiN film deposited on Si substrate are clearly show on the EDX spectrum (Figure 4) indicated by red color for thinner film. Similarly, we have found Ti, and N elements for TiN/Si for thicker film (black color).

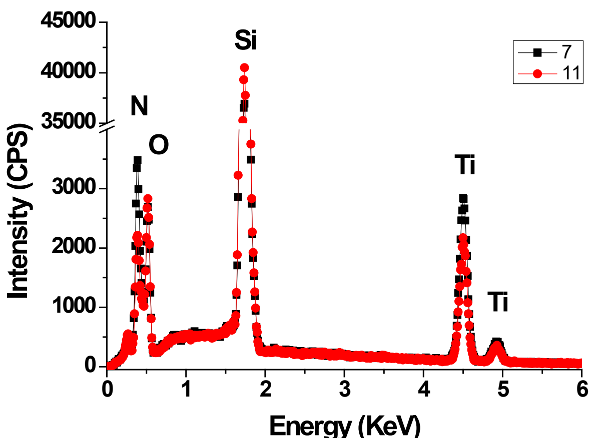

Fig. 5. EDX spectra for TiN/Si (thicker film at red color) and TiN/Si (thinner film at black color) deposited by DC magnetron sputtering.

The titanium nitride [6] film has shown that the Ti and N were major elements and the composition was under stoichiometry. Table 1 shows that the ratio (N/Ti) was about 0.5 confirm that the films are near stoichiometry which become consisted with XRD results.

Table 1. The EDX result (weight and atomic percentage) for TiN/Si deposited at 5 min and 20 min.

sample	N	Ti	N/Ti
TiN11/Si (5 min)	30.67	69.33	0.44
TiN7/Si (20 min)	36.47	63.53	0.57

3.5 Corrosion measurements

3.5.1 Potentiodynamic polarization - Tafel method

The characteristic electrochemical parameters in Tafel method [24], include corrosion potential (E_{corr}) and corrosion current density (I_{corr}). The corrosion current density attained from the polarization curves is usually proportional to the corrosion rate [25]. The corrosion resistance of TiN films deposited on SS304 in 3.5 NaCl % solutions (equivalent seawater) was studied and compared with uncoated SS304 sample.

Table 2 summarized the I_{corr}, and E_{corr} corrosion for substrate LCS and films. The I_{corr}increases from 61.5 μA/cm² to 164.9 μA/cm² for TiN/ LCS with increase the thickness (time) from 125 nm to 500 nm due to increase the roughness (bigger grain size), and the corrosion rate increase from 0.6 mm/year to 1.5 mm/year, respectively. The better corrosion resistance corresponds the thinner film (smaller grain size and lower roughness), so in all cases, the film (TiN/LCS) has better the LCS reference (without coating), because the corrosion rate for LCS was higher than TiN films and it was about 547 mm/year. This result was in a good agreement with recent work [26], where we have investigated the CrN/SS304 corrosion behavior and with another study using TiAlV film. Recent studies have shown that grain size is a critical factor in the corrosion resistance of metallic materials and mechanical properties [27-29], where smaller grain size is associated with better corrosion resistance.

Table 2. Corrosion potential (E_{corr}) and corrosion of TiN films as well as for LCS (reference) by Tafel extrapolation method in 3.5% NaCl solution at 25 °C.

Samples	I_{corr} (μA/cm²)	E_{corr} (mV)
TiN8/LCS (5 min)	61.5	-587.1
TiN10/LCS (10 min)	74.42	-592.1
TiN3/LCS (15 min)	118.5	-649.2 mV
TiN2/LCS (20 min)	164.9	-630.4 mV
LCS (non coated samples)	60.11	-591.9

Figure 6a shows potentiodynamic polarization curves (a), (b), (c) and (d) for TiN films. Similarly, the Figure 6e present potentiodynamic polarization for LCS substrate in 3.5% NaCl at 25°C. It can be seen that the corrosion properties have been improved as mentioned above. The smallest corrosion current density corresponds to the best corrosion properties was obtained for the TiAlVN film prepared, the TiN film stayed better than SS304 (without film). A positive value of the corrosion potential is an indicator of low electrochemical activity that is associated with good corrosion resistance [30].

The corrosion resistance of the sample has been enhanced in comparison with the reference (SS304). All the coated samples have shown less corrosion current density I_{corr} and lower corrosion rate than the reference samples (Figure 6).

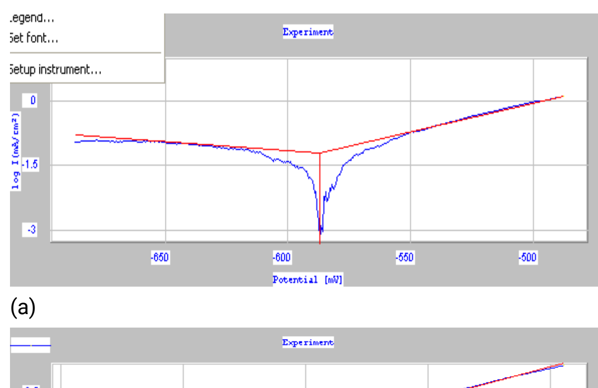

(a)

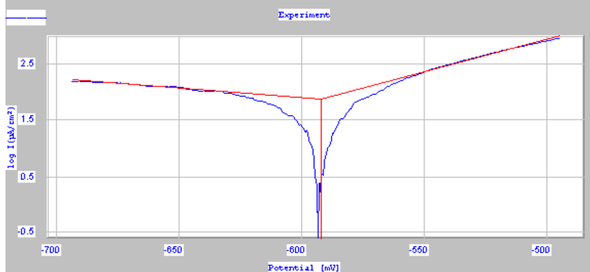

(b)

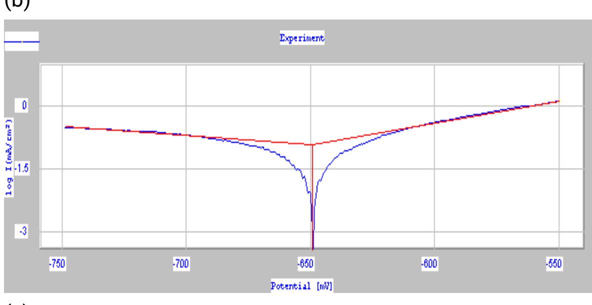

(c)

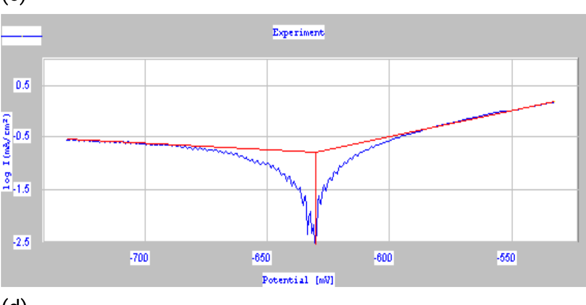

(d)

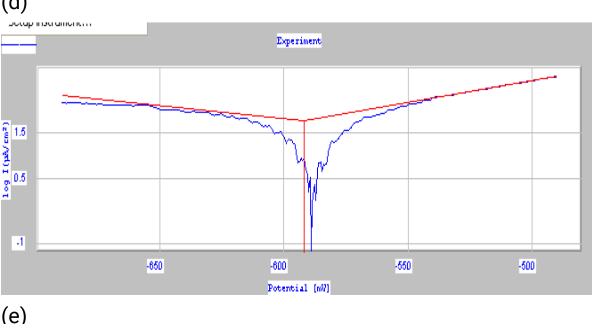

(e)

Fig. 6. Potentiodynamic polarization curves for TiN films deposited (a) at 5 min, (b) 10 min, (c) 15 min and (d) at 20 min, and (e) for LCS reference in 3.5% NaCl at 25 °C.

We have found in a previous work, where X-ray photoelectron spectroscopy (XPS) was used to study the chemical composition of the passive layer formed on the films deposited by vacuum arc discharge method, that this layer was mainly composed of TiO_2 [4]. Many factors could influence corrosion behavior such as TiO_2 phase, stoichiometry, defect density, preferred orientation, phases and crystalline quality [31].

Table 3 shows I_{corr}, and E_{corr} corrosion for and film deposited on SS304 at min, which has the lower value of roughness (as mentioned above in AFM measurement) and substrate SS304 (noncoated). The I_{corr}forTiN/SS304 (13.1 μA/cm²) is less than SS304 substrate (16.5 μA/cm²) which indicates that the film has better corrosion resistance than SS304 substrate. So, the corrosion rate for film (TiN/SS) has lower than the SS304 reference (without coating), because it has been 119 mm/year and 150 mm/year, respectively; The deposited film resist the corrosive media (3.5% NaCl solution) better than SS304 substrate, this accorded with behaviors our film deposited on LCS substrate.

Table 3. corrosion potential (E_{corr}) and corrosion of TiN film deposited at 5 min and for SS304 (reference) by Tafel extrapolation method in 3.5% NaCl solution at 25ºC.

	Icorr (μA/cm²)	Ecorr (mV)
TiN14/SS304 (5 min)	13.1	539.0
SS304	16.5	-416.4

The Figure 7 shows potentiodynamic polarization curves (a) for TiN/SS304 film deposited at 5 min and (e) for SS304 reference, I_{corr} of the TiN film smaller than SSS304 which confirm latter paragraph.

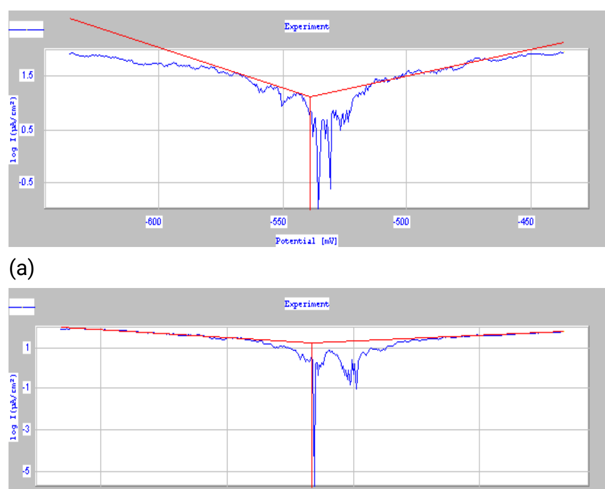

(a)

(b)

Fig. 7. Potentiodynamic polarization curves (a) for TiN/SS304 film deposited at 5 min and (e) for SS304 reference in 3.5% NaCl at 25 °C.

For the frequency bandwidth, the impedance (EIS) is presented by the Nyquist plots. It is useful and effective technique for verifying the corrosion behavior of thin films [32]. The experimental curves are fitted after selecting the suitable circuit using EC-Lab impedance program (Figure 8). The impedance parameters, R1, R2 and R3 indicating the resistance of the solution, coating and coating/substrate interface, respectively. Also, the polarization resistance Rp= (R2+R3) were calculated from Nyquist plots.

Figure 8 shows the experimental plots for TiN/SS304 film (deposited at 5 min) and the reference SS304, we found the resistance of the film is better than the reference (SS304), where the resistance of film (about 1596.9 Ω.cm^2) is higher than SS304 (about 1439 Ω.cm^2). This result was in a good agreement with Tafel plots (potentiodynamic test).

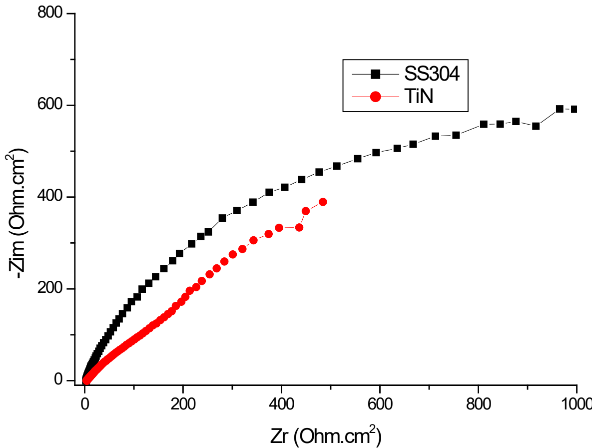

Fig. 8. Nyquist plots for film TiN/SS304 deposited at 5 min and for SS304 substrate.

3.6 Optical microscope study

Figure 9 show images of optical microscope for LCS substrate (a) before corrosion and (b) at magnification of 500x. Images of optical microscope for SS304 substrate (c) before corrosion and (d) at magnification 500x.

Figure 9 shows the morphology for samples LCS (9-b) and (9-d) for SS304 500x after corrosion test, where there were petting. It was large scale (or area) for LCS sample and small for SSS304, which confirmed that the SS304 exhibit resistance to corrosion more than the LCS sample. This is consistence with corrosion current density I_{corr} as well as with corrosion rate measured by Tafel method (figures 6 and 7).

Similarly, Figure 10 shows images optical microscope for TiN/LCS film deposited at 5 min after corrosion (a) at 500x magnification and (b) at 1200x magnification. Images optical microscope for TiNSS304 film (c) at 500x magnification and (d) at 1200x magnification. The corrosion petting was larger (or area for TiN/LCS sample) than TiN/SSS304 due to the quality of SS304 which better than LCS and it could help the film to resist the corrosive media. This result shows that the TiN exhibit good corrosion resistance than SS304 and LCS samples (without coating). There is consistence with corrosion current density I_{corr} as well as with corrosion rate which small for coated samples using Tafel method (as mentioned above).

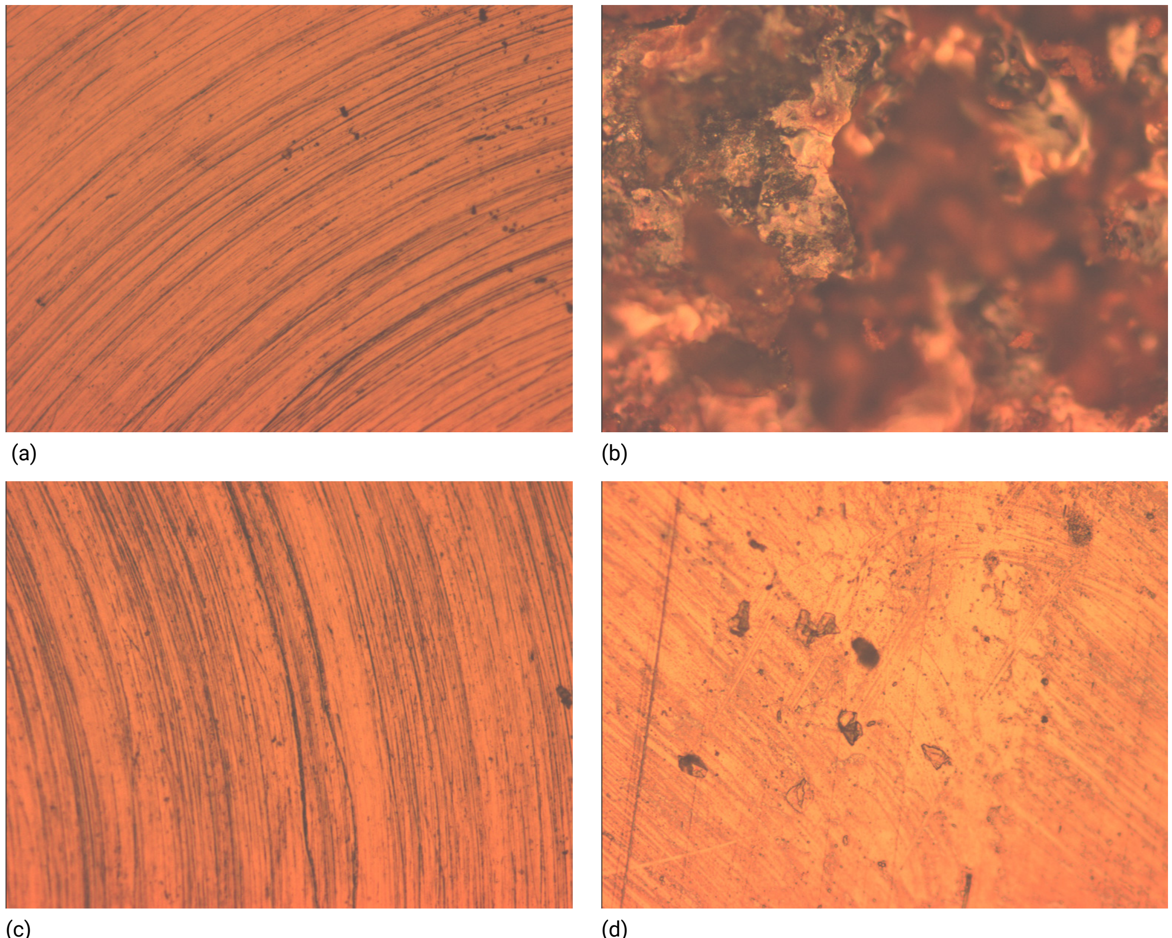

Fig. 9. Images optical microscope for LCS substrate (a) before corrosion and (b) at magnification 500x. Images optical microscope for SS304 substrate (c) before corrosion and (d) at magnification 500x.

It has been reported that refinement of grain size has remarkable enhancement in the corrosion resistance [33, 34]. This agrees with our results where the smaller grain size according with better corrosion resistance, as it can be seen in figures 6, 7 and 9.

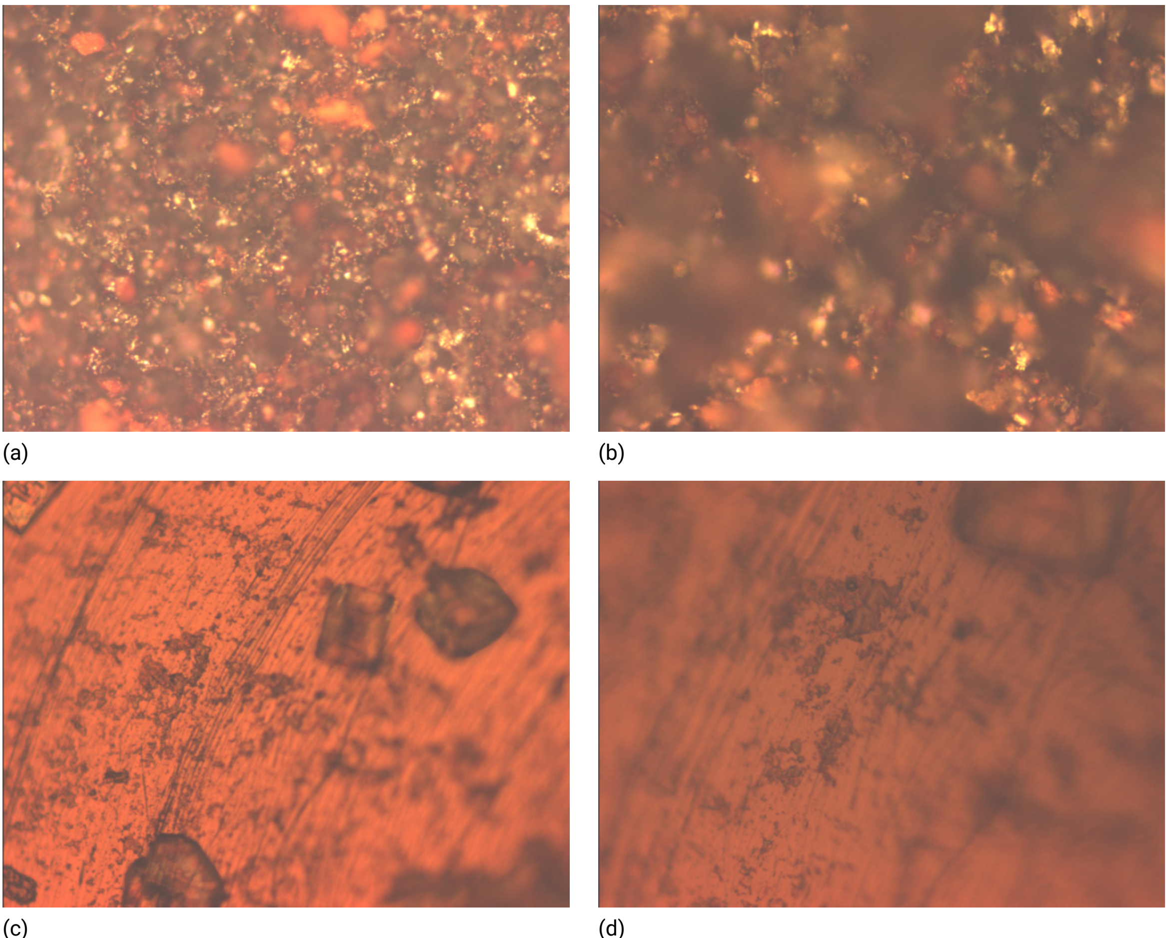

Fig. 10. Images optical microscope for TiN/LCS film at 5 min after corrosion (a) at 500x magnification and (b) at 1200x magnification. Images optical microscope for TiN/SS304 film (c) at 500k magnification and (d) at 1200x magnification.

4. Conclusions

TiN thin films have been synthesized by DC magnetron sputtering technique at different substrates at 100 °C. SEM images were used to measure the thickness of the deposited film on Si substrate, and it was found increase in the thickness with the deposition time. The Vickers microhardness value was measured for TiN films deposited on Si and on SS304. The composition of the films has been examined by EDX technique, to verify the elementary percentages, where the N/Ti ratio was about 0.5 with low oxygen contamination. We found strong dependence between roughness (measured by AFM, optical microscope and SEM), XRD measurement (grain size) and corrosion. The decrease of the roughness consequently improves resistance proprieties using potentiodynamic (Tafel) and the impedance (EIS) methods. They indicated that the films resist the aggressive action in seawater (corrosion media). Therefore, titanium nitride film, especially the smooth one, is an effective method to enhance the corrosion resistance of LCS as well as SS304 references (noncoated samples).

Acknowledgments

Authors would like to thank Dr. I. Othman, the Director General of AECS for support, Dr. M.D Zidan for valuable discussion.

Author Contributions

B. Abdallah: Conceptualization, Methodology, Writing, and Supervision; M. Kakhia: Methodology and Investigation; W. Alsadat: Investigation; W. Zetun: Investigation and Editing; A. Hijazy: Investigation.

References and Notes

[1] Gurrappa, I. *Mater. Charact*. **2003**, *51*, 131. [Crossref]

[2] Faria, A. C. L.; Rodrigues, R. C. S.; Claro, A. P. R. A.; de Mattos, M. G. C.; Ribeiro, R. F. *J. Mech. Behav. Biomed. Mater*. **2011**, *4*, 1873. [Crossref]

[3] Metikoš-Huković, M.; Kwokal, A.; Piljac, J. *Biomaterials* **2003**, *24*, 3765. [Crossref]

[4] Abdallah, B.; Mrad, O.; Ismail, I. M. *Acta Phys. Polonica A*. **2013**, *123*, 76. [Crossref]

[5] Abdallah, B.; Kakhia, M.; Alssadat, W.; Rihawy, M. S. *Iranian J. Sci. Technol. Trans. A Sci*. **2019**, *4*, 1957. [Crossref]

[6] Zhang, H.; Duoa, S.; Xu, X.; Liu, T. *Key Eng. Mater*. **2014**, *591*, 95. [Crossref]

[7] Pohrelyuk, I. M.; O. V.; TkachukProskurnyak, R. V. *ISRN Corrosion* **2013**, *ID 241830*, 1. [Crossref]

[8] Subramanian, B.; Ananthakumar, R.; Jayachandran,

M. *Vacuum* **2010**, *85*, 601. [Crossref]

[9] Ismail, I. M.; Abdallah, B.; Abou-Kharroub, M.; Mrad, O. *Nucl. Instr. Meth. B*. **2012**, *271*, 102. [Crossref]

[10] Abdallah, B.; Naddaf, M.; Abou-Kharroub, M. *Nucl. Instr. Meth. B*. **2013**, *298*, 55. [Crossref]

[11] Naddaf, M.; Abdallah, B.; Ahmad, M.; A-Kharroub, M. *Nucl. Instr. Meth. B*. **2016**, *381*, 90. [Crossref]

[12] Filip, R. *Arch. Mater. Sci. Eng.* **2008**, *30*, 25.

[13] Oh, D.-J.; Kim, H.-J.; Chung, C.-H. *J. Korean Acad. Prosthodont*. **2006**, *44*, 740.

[14] Ribeiro, E.; Malczyk, A.; Carvalhoa, S.; Rebouta, L.; Fernandes, J. V.; Alves, E., et al. *Surf. Coat Tech.* **2002**, *151, 152*, 515. [Crossref]

[15] Abdallah, B.; Jazmati, A. K.; Refaaia, R. *Mater. Res*. **2017**, 1. [Crossref]

[16] Alyones, J.; Salameh, M.; Abdallah, B. *Silicon* **2020**, *12*, 2489. [Crossref]

[17] Abdallah, B.; Duquenne, C.; Besland, M. P.; Gautron, E.; Jouan, P. Y.; Tessier, P. Y.; et al. *Eur. Phys. J. Appl. Phys*. **2008**, *43*, 309. [Crossref]

[18] Jazmati, A. K.; Abdallah, B. *Mater. Res*. **2018**, *21*, 1. [Crossref]

[19] Abdallah, B.; Kakhia, M.; Alsadat, W. *Int. J. Mater. Struct. Integr.* **2019**, *11*, 1.[Crossref]

[20] Danışman, Ş.; Savaş, S.; Topal, E. S. *Tribol. Ind.* **2008**, *30*, 17.

[21] Alkhawwam, A.; Abdallah, B.; Jazmati, A. K.; Tootanji, M.; Lahlah, F. *Surf. Rev. Lett.* **2019**, *1950188*. [Crossref]

[22] Al-Khawaja, S.; Abdallah, B.; Abou Shaker, S.; Kakhia, M. *Compos. Interfaces* **2015**, *22*, 221. [Crossref]

[23] Abdallah, B.; Jazmati, A. K.; Nounou, F. *J. Nanostruct*. **2020**, *10*, 185. [Crossref]

[24] Frankel, G. S. Fundamentals of Corrosion Kinetics. In: Hughes AE, Mol JMC, Zheludkevich ML, Buchheit RG, editors. Active Protective Coatings: New-Generation Coatings for Metals. Dordrecht: Springer Netherlands; 2016. p. 17.

[25] Wang, Z. B.; Lu, J.; Lu, K. *Surf. Coat Tech*. **2006**, *201*, 2796. [Crossref]

[26] Abdallah, B.; Jazmati, A. K.; Kakhia, M. *Optik* **2018**, *158*, 1113. [Crossref]

[27] Unal, O.; CahitKaraoglanli, A.; Varol, R.; Kobayashi, A. *Vacuum* **2014**, *110*, 202. [Crossref]

[28] Mao, X. Y.; Li, D. Y.; Fang, F.; Tan, R. S.; Jiang, J. Q. *Wear* **2011**, *271*, 1224. [Crossref]

[29] Wang, T.; Yu, J.; Dong, B. *Surf. Coat Tech*. **2006**, *200*, 4777. [Crossref]

[30] Kalisz, M.; Grobelny, M.; Świniarski, M.; Mazur, M.; Wojcieszak, D.; Zdrojek, M.; et al. *Surf. Coat Tech.* **2016**, *290*, 124. [Crossref]

[31] Musil, J. *Surf. Coat Tech.* **2000**, *125*, 322. [Crossref]

[32] Song, G.-H.; Yang, X.-P.; Xiong, G.-L.; Lou, Z.; Chen, L.-J. *Vacuum* **2013**, *89*, 136. [Crossref]

[33] Op't Hoog, C.; Birbilis, N.; Estrin, Y. *Adv. Eng. Mater*. **2008**, *10*, 579. [Crossref]

[34] Aung, N. N.; Zhou, W. *Corros. Sci*. **2010**, *52*, 589. [Crossref]

How to cite this article

Abdallah, B.; Kakhia, M.; Alsadat, W.; Zetun, W.; Hijazy, A. *Orbital: Electron. J. Chem.* **2021**, *13*, 69. http://dx.doi.org/10.17807/orbital.v13i1.1577